Report

Cell Reports

Plasticity between Epithelial and Mesenchymal States Unlinks EMT from Metastasis-Enhancing Stem Cell Capacity

Graphical Abstract

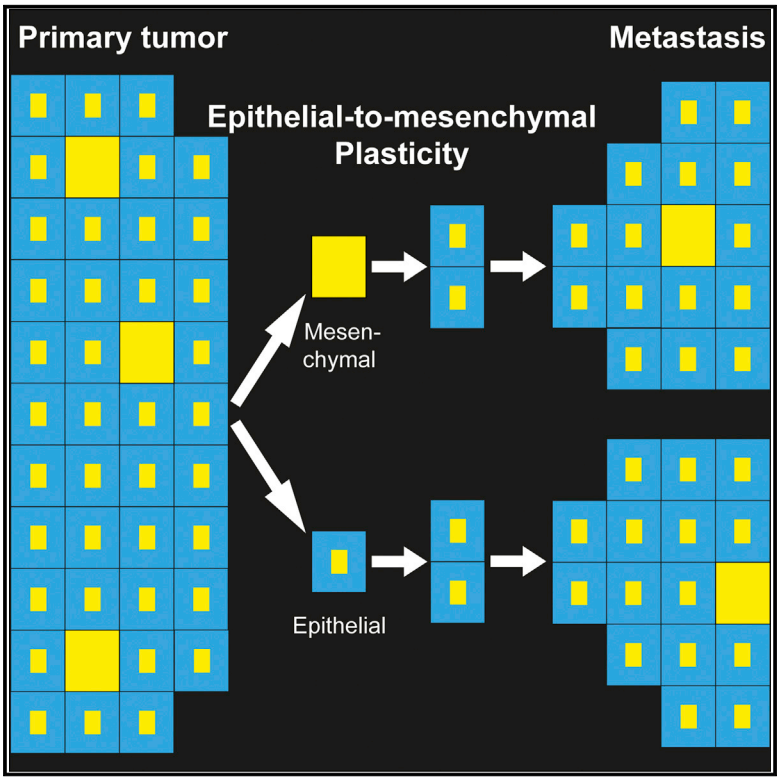

Highlights

- Direct evidence of EMT obtained in unperturbed breast tumors by real-time visualization
- EMT exists in breast tumors without experimentally altering EMT inducers
- Tumor cells that underwent EMT are the migratory cells within a tumor
- Outgrowth potential differences between states are irrelevant due to plasticity

Authors

Evelyne Beerling, Daniëlle Seinstra, Elzo de Wit, ..., Alexander van Oudenaarden, Nienke Vrisekoop, Jacco van Rheenen

Correspondence

n.vrisekoop@umcutrecht.nl (N.V.), j.vanrheenen@hubrecht.eu (J.v.R.)

In Brief

Beerling et al. identified a previously undetectable pool of cells in epithelial breast tumors that have undergone EMT without experimental induction. These cells are motile when disseminating and revert back to the epithelial state upon metastatic outgrowth. This epithelial-mesenchymal plasticity equalizes metastatic outgrowth potential between epithelial and mesenchymal tumor cells.

Accession Numbers

GSE77107
PRJEB5939

Beerling et al., 2016, Cell Reports *14*, 1–8
March 15, 2016
http://dx.doi.org/10.1016/j.celrep.2016.02.034

CellPress

Please cite this article in press as: Beerling et al., Plasticity between Epithelial and Mesenchymal States Unlinks EMT from Metastasis-Enhancing Stem Cell Capacity, Cell Reports (2016), http://dx.doi.org/10.1016/j.celrep.2016.02.034

Cell Reports
Report

Plasticity between Epithelial and Mesenchymal States Unlinks EMT from Metastasis-Enhancing Stem Cell Capacity

Evelyne Beerling,[1,4] Daniëlle Seinstra,[1,4] Elzo de Wit,[1,3] Lennart Kester,[1] Daphne van der Velden,[3] Carrie Maynard,[1] Ronny Schäfer,[1] Paul van Diest,[2] Emile Voest,[3] Alexander van Oudenaarden,[1] Nienke Vrisekoop,[1,5,*] and Jacco van Rheenen[1,*]

[1]Cancer Genomics Center-Hubrecht Institute-KNAW & University Medical Centre Utrecht, Uppsalalaan 8, 3584 CT Utrecht, the Netherlands
[2]Department of Pathology, University Medical Centre Utrecht, Heidelberglaan 100, 3584 CX Utrecht, the Netherlands
[3]Netherlands Cancer Institute, Plesmanlaan 121, 1066 CX Amsterdam, the Netherlands
[4]Co-first author
[5]Present address: Laboratory of Translational Immunology, Department of Pulmonary Diseases, University Medical Centre Utrecht, Lundlaan 6, 3584 EA Utrecht, the Netherlands
*Correspondence: n.vrisekoop@umcutrecht.nl (N.V.), j.vanrheenen@hubrecht.eu (J.v.R.)
http://dx.doi.org/10.1016/j.celrep.2016.02.034

SUMMARY

Forced overexpression and/or downregulation of proteins regulating epithelial-to-mesenchymal transition (EMT) has been reported to alter metastasis by changing migration and stem cell capacity of tumor cells. However, these manipulations artificially keep cells in fixed states, while in vivo cells may adapt transient and reversible states. Here, we have tested the existence and role of epithelial-mesenchymal plasticity in metastasis of mammary tumors without artificially modifying EMT regulators. In these tumors, we found by intravital microscopy that the motile tumor cells have undergone EMT, while their epithelial counterparts were not migratory. Moreover, we found that epithelial-mesenchymal plasticity renders any EMT-induced stemness differences, as reported previously, irrelevant for metastatic outgrowth, because mesenchymal cells that arrive at secondary sites convert to the epithelial state within one or two divisions, thereby obtaining the same stem cell potential as their arrived epithelial counterparts. We conclude that epithelial-mesenchymal plasticity supports migration but additionally eliminates stemness-enhanced metastatic outgrowth differences.

INTRODUCTION

Metastatic growth is the major cause of cancer-associated mortality. To successfully grow metastases, epithelial tumor cells need to acquire invasive properties to disseminate and stem cell properties to grow new tumors at distant sites (Hanahan and Weinberg, 2011). Metastasizing cancer cells have been suggested to hijack a developmental program named epithelial-to-mesenchymal transition (EMT) (Bill and Christofori, 2015; Kalluri and Weinberg, 2009; Lim and Thiery, 2012). During developmental EMT, cells lose cell-cell contacts and concomitantly decrease the expression of the epithelial adherens junction molecule E-cadherin (E-cad) and gain expression of proteins involved in, e.g., invasion and stemness (Kalluri and Weinberg, 2009; Lim and Thiery, 2012; Thiery and Sleeman, 2006).

The effect of EMT on stemness, as well as the role and even the very existence of EMT during metastasis, are heavily debated (Del Pozo Martin et al., 2015; Fischer et al., 2015; Zheng et al., 2015). For example, contradicting findings were published on the stem cell potential of tumor cells with an epithelial or mesenchymal state. Some studies found that EMT-inducing transcription factors, such as Twist, coincide with the acquisition of stem cell properties, thereby supporting metastatic growth (Mani et al., 2008; Morel et al., 2008; Wellner et al., 2009; Yang et al., 2004). Other studies found that a forced reversion to an epithelial state through Twist knockdown leads to metastasis-initiating abilities (Ocaña et al., 2012; Tsai et al., 2012). Importantly, both experimental approaches may not represent the true in vivo status of cells because they require gene manipulations that artificially force cells into fixed states, while in vivo cells may be able to transiently and reversibly switch between states, a process that from here on is referred to as epithelial-mesenchymal plasticity. Moreover, the non-physiological overexpression or complete loss of EMT-regulators, such as Twist1, may induce expression profiles and subsequently stem cell phenotypes that do not exist under physiological conditions. Finally, EMT regulators can have oncogenic functions independently of their ability to induce EMT, thus observed phenotypes that result from gene manipulation may not be exclusively due to EMT induction (Beck et al., 2015). These data and concerns illustrate the importance of studying EMT in non-manipulated in vivo settings.

Although EMT would best be studied in the physiological in vivo settings, non-experimentally induced EMT during metastasis has yet to be observed. For example, extensive histological examination of human invasive ductal mammary carcinomas

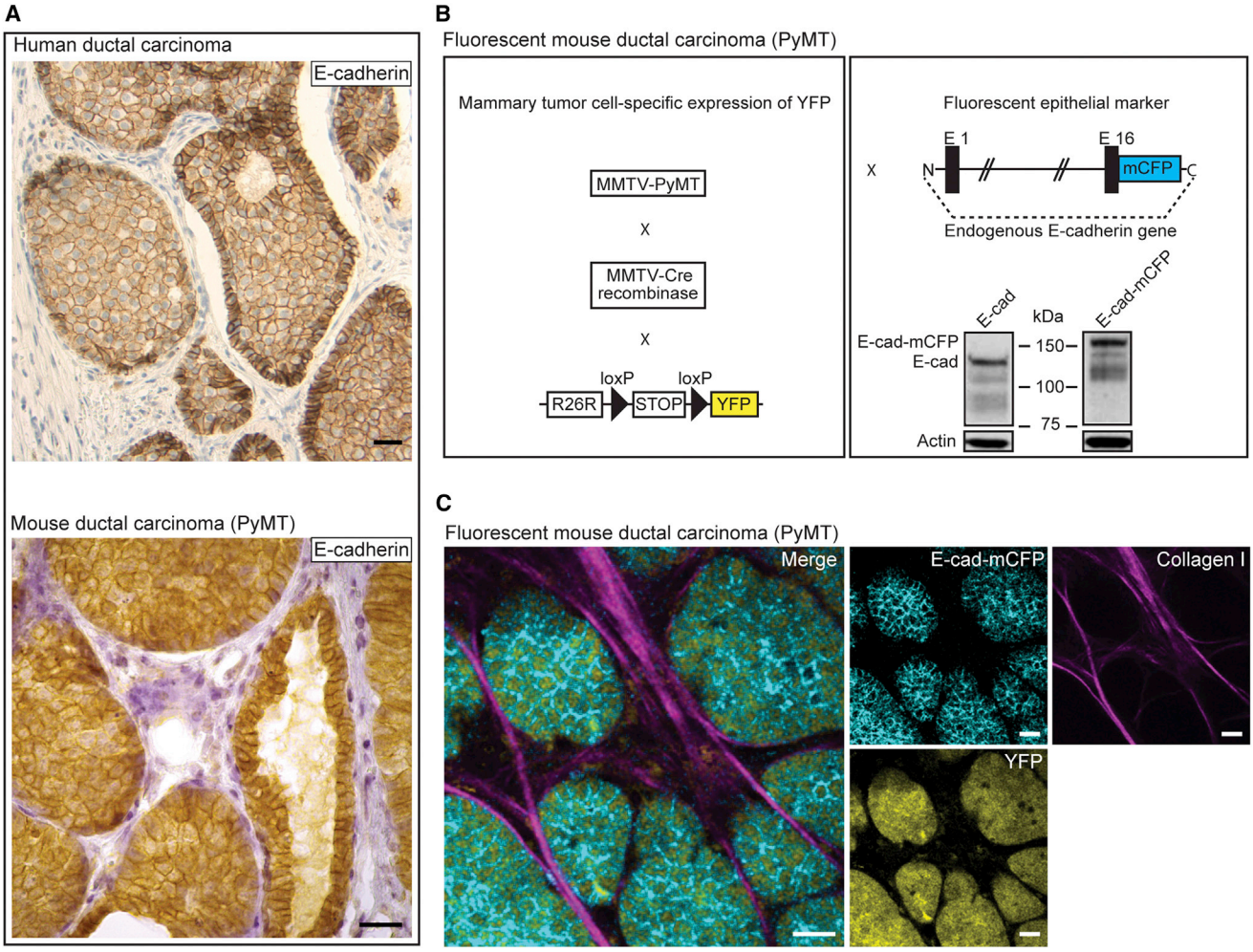

Figure 1. Development of a Fluorescent Mouse Model for Metastatic E-cad-Positive Invasive Ductal Carcinomas

(A) Human invasive ductal carcinoma (upper) and a late-stage MMTV-PyMT tumor (lower), stained for E-cad and counterstained with H&E. Scale bar, 30 μm.

(B) Schematic representation of the fluorescent mouse model in which all tumor cells express YFP and in which the endogenous E-cad is labeled with CFP. The western blot shows wild-type and CFP-tagged E-cad.

(C) Multi-photon images of fluorescent PyMT mammary tumors. Scale bars, 30 μm.

shows that, even in tumors that have metastasized, tumor cells in the primary tumor, as well as the metastases, display an epithelial phenotype (e.g., Bukholm et al., 2000; Jeschke et al., 2007; Kowalski et al., 2003). This means that either EMT does not exist when it is not experimentally induced or EMT remains undetected in these static images because only a small population of cells temporarily adapts a mesenchymal state. Therefore, in addition to the development of models in which EMT can occur without modifying EMT-regulators, techniques are required that are able to reveal and study the potentially rare and undetectable pool of cells going through EMT.

Here, we combine high-resolution intravital imaging, single-cell sequencing, and transplantation techniques to investigate the role of EMT and epithelial-mesenchymal plasticity in metastasis of invasive ductal carcinomas. Our data suggest that epithelial-mesenchymal plasticity supports tumor cell migration and causes metastasis-enhancing stem cell capacity differences between epithelial and mesenchymal states to be irrelevant.

RESULTS AND DISCUSSION

To determine whether EMT occurs without artificial induction, we used polyomavirus middle T antigen (PyMT) mice that develop ductal mammary carcinomas that recapitulate the progression of human mammary adenoma to late carcinoma stages and metastasize primarily to lymph nodes, lungs, and, occasionally, liver (Guy et al., 1992; Lin et al., 2003; Welm et al., 2007). Similar to human ductal carcinomas, these mammary tumors highly express E-cad, even in the late carcinoma stage and metastases (Figure 1A). To visualize EMT in vivo, we crossed these *MMTV-PyMT* mice with *MMTV-Cre* and *R26R-loxP-stop-loxP-YFP* (*R26R-YFP*) mice (Srinivas et al., 2001) to specifically label all tumor cells with yellow fluorescent protein (YFP). Next, we crossed

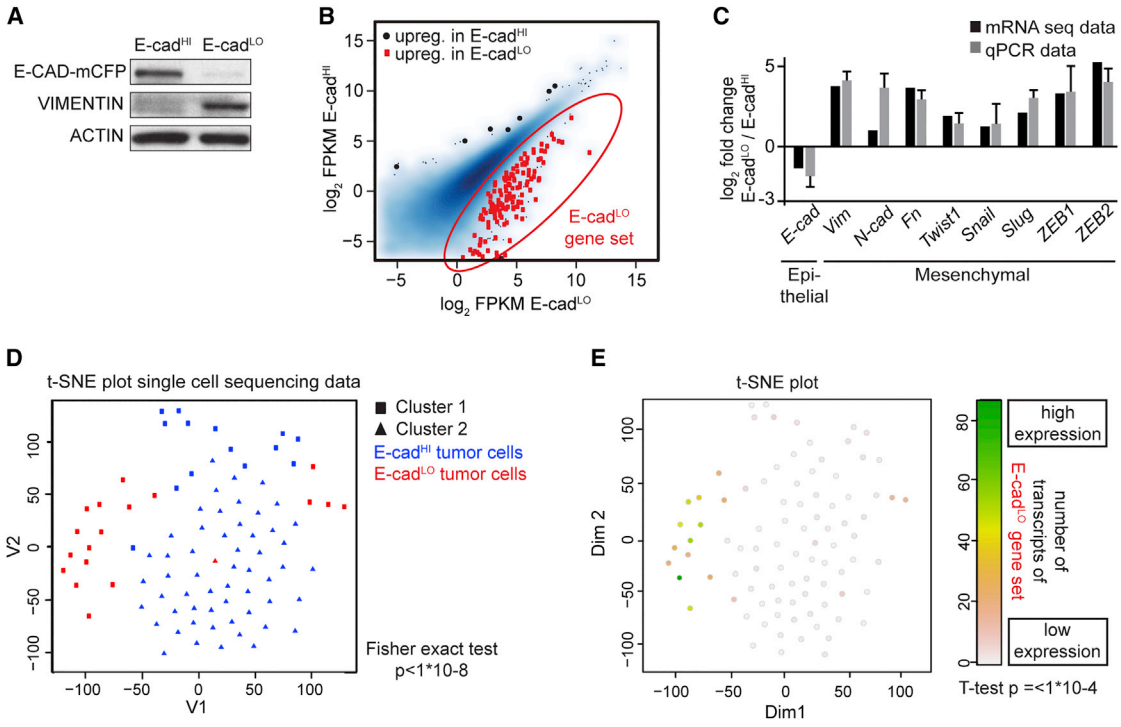

Figure 2. Rare E-cad^{LO} Cells Isolated from Mouse Invasive Ductal Carcinomas Have Undergone EMT

(A) Western blot of indicated samples. n = 3 mice.

(B) Scatterplot showing expression values for E-cad^{HI} and E-cad^{LO} cells. Red dots that are encircled in red represent genes that are significantly upregulated in E-cad^{LO} cells (q value < 0.01).

(C) The relative mRNA expression of EMT-related genes determined by RNA sequencing (RNA-seq) and RT. n = 4 mice, except for ZEB1, where n = 3 mice.

(D) T-distributed stochastic neighbor embedding (t-SNE) plot. Using unsupervised K-medoids clustering, two separate clusters were identified indicated as squares and triangles that overlap with E-cad^{HI} (blue) and E-cad^{LO} (red) tumor cells.

(E) t-SNE intensity plot for genes differentially upregulated in (B).

Related to Figures S1, S2, and S3 and Table S1.

these animals with *E-cad-mCFP* mice in which a monomeric cyan fluorescent protein (mCFP) is fused to endogenous E-cad (Snippert et al., 2010), in order to label all endogenous E-cad with mCFP (Figure 1B). The resultant *MMTV-PyMT; MMTV-Cre; R26R-YFP; E-cad-mCFP* animals develop ductal mammary tumors and metastases in which all tumor cells are YFP-labeled and endogenous E-cad is tagged with mCFP (Figure 1C). Microscopic inspection (Figure 1C) and flow cytometry (Figure S1) of these fluorescent tumors showed that the vast majority of cells appear to have high levels of membrane-localized E-cad (E-cad^{HI} cells).

To test whether these tumors also contain a population of tumor cells that have undergone EMT in which E-cad is not functional by either downregulation of the expression or by decreasing membrane-localized E-cad, we dissociated fluorescent PyMT tumors and exposed the extracellular domain of E-cad to a fluorescently labeled antibody. We sorted YFP-expressing tumor cells, excluding, for example, lymphocytes (see Figure S1). In contrast to analysis of histological images, careful analysis of the flow cytometry data showed that in addition to the population of E-cad^{HI} tumor cells another, much smaller population of tumor cells could be found. In this population the expression of E-cad-mCFP was low and/or E-cad was non-functional due to intracellular localization as determined by low extracellular antibody staining (E-cad^{LO}; Figure S1B). Western blot analysis confirmed that E-cad^{LO} cells have low levels of E-CAD and a concomitant upregulation of VIMENTIN (Figure 2A), which is consistent with mesenchymal characteristics (Kalluri and Weinberg, 2009). Moreover, using mRNA deep sequencing, we observed differential expression in the E-cad^{HI} and E-cad^{LO} cells of typical EMT genes, such as *Vimentin*, *Fibronectin*, and *N-cadherin*, and transcription factors that regulate EMT, including *Snail*, *Slug*, *Twist*, *ZEB1*, and *ZEB2*, referred to as the E-cad^{LO} gene set (Figures 2B and 2C; Table S1). These results were confirmed by qPCR (Figures 2C and S2A).

These data show that in our system E-cad status can be used to distinguish between epithelial and mesenchymal phenotypes on the population level. To test whether this holds true at the single-cell level, we performed single-cell mRNA sequencing of 72 E-cad^{HI} and 25 E-cad^{LO} cells. When performing unsupervised K-medoids clustering of the individual expression profiles, two separate clusters were identified that overlapped with the E-cad^{HI} and E-cad^{LO} cells (Figure 2D; $p < 1^{-8}$). The single E-cad^{LO} cells had higher expression of the E-cad^{LO} gene set from the bulk sequencing data, confirming the mesenchymal identity of the E-cad^{LO} cells on the single-cell level (Figure 2E;

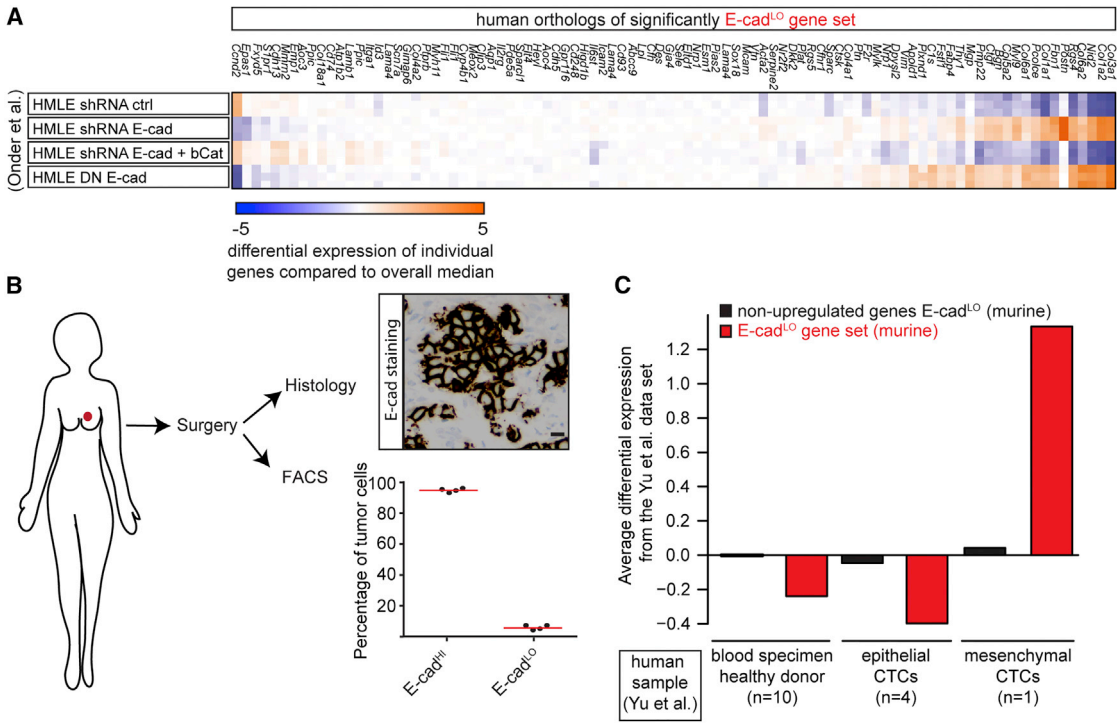

Figure 3. E-cad^{LO} Cells Are Similar to Human Mesenchymal Tumor Cells

(A) From a published dataset (Onder et al., 2008), the expression level in human mammary epithelial cells (HMLE) of the human orthologs of the mouse E-cad^{LO} gene set in Figure 2B was retrieved. Differential expression levels per gene as the deviation of the median across all experiments are shown.

(B) The image shows an E-cad^{+} human invasive ductal carcinoma, and the graph shows the percentage of E-cad^{HI} and E-cad^{LO} cells (n = 4 tumors). Scale bar, 20 μm.

(C) From published RNA-seq experiments of human breast cancer CTCs (Yu et al., 2013), the relative expression levels of human-mouse orthologs were retrieved. Plots show the average differential expression found in the Yu et al. (2013) dataset for the E-cad^{LO}-upregulated (red bars) or non-upregulated genes (black bars). Expression levels for circulating cells were determined for blood draws from ten healthy donors (left two bars), four blood draws from one patient with CTCs with an epithelial phenotype (middle two bars), and one of the same patient with CTCs with a mesenchymal phenotype (right two bars).

t test $p < 1^{-4}$; Figures S2B and S2C). Furthermore, E-cad^{LO} and E-cad^{HI} cells clustered separately in a heatmap (Figure S2D), and we observed that the expression profiles of E-cad^{HI} cells were more similar to each other (Pearson correlation of 0.45) than to the profiles of E-cad^{LO} cells (Pearson correlation of 0.35, Wilcoxon two-sided test = $p < 10^{-15}$; Figures 2D and S2D). Collectively, these data show that in PyMT tumors at the single-cell level that E-cad status can be used to discriminate between cells with epithelial and mesenchymal features.

Next, we tested whether human tumors also contain E-cad^{LO} cells. As a first indication, we found that the E-cad^{LO} gene set (marked with red dots in Figure 2B) is upregulated in human cells in which EMT is induced upon E-cad knockdown or expression of dominant-negative E-cad (Onder et al., 2008) (Figure 3A, $p <$ 0.0001 hypergeometric test). Next, we obtained tumors directly after patients underwent mastectomy and selected four tumors that stained positive for E-cad on histological sections (Figure 3B). We dissociated the tumors into single cells, stained the cells with DAPI to exclude apoptotic cells, EpCAM to select for tumor cells (Yu et al., 2013), and E-cad to distinguish between E-cad^{HI} and E-cad^{LO} cells. By flow cytometry we indeed detected both E-cad^{HI} and E-cad^{LO} cells (Figure 3B). To test whether human E-cad^{LO} and mouse E-cad^{LO} cells are similar, we used a recently published dataset of gene expression in epithelial- and mesenchymal-circulating tumor cells (CTCs) from breast cancer patients (Yu et al., 2013). Importantly, the mouse E-cad^{LO} gene set was also upregulated in the human mesenchymal CTCs, but not in the human epithelial CTCs or in healthy blood specimens (Figure 3C). Combined, these results show that we have identified a subpopulation of mouse tumor cells (E-cad^{LO}) that is similar to that of human mesenchymal CTCs.

Since tumors are genetically very heterogeneous, the E-cad^{LO} CTCs from breast cancer patients and from our mouse model may either adapt a permanent mesenchymal state by, e.g., mutations in EMT-regulators, or represent a transient reversible mesenchymal state. To test whether the mesenchymal state is reversible, we first generated organoids from the *MMTV-PyMT; MMTV-Cre; R26R-YFP; E-cad-mCFP* carcinomas. We stimulated these organoids with transforming growth factor beta (TGF-beta) and hepatocyte growth factor (HGF) and indeed observed an increase in the number of E-cad^{LO} cells (Figure S3A), showing that the mesenchymal state of E-cad^{LO} cells can be stimulated. This state can also be lost, since orthotopic transplantation of E-cad^{LO} cells always resulted in mammary tumors containing tumor cells with a predominantly epithelial

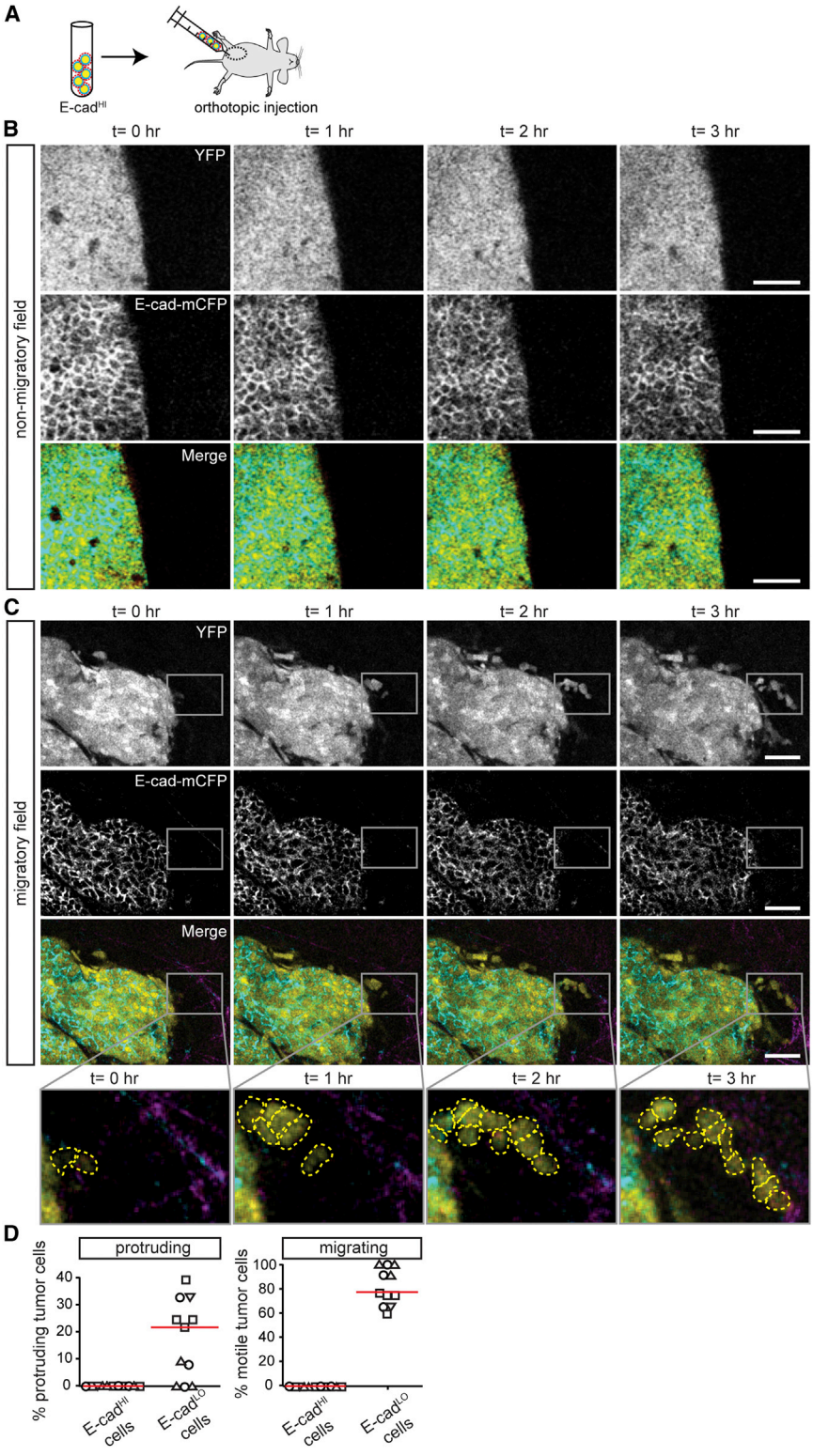

Figure 4. Behavioral Characterization of Rare E-cad^{LO} Tumor Cells in Mouse Mammary Carcinomas that Highly Express E-cad

(A) Cartoon of the experimental setup.

(B and C) Intravital images of PyMT tumors containing non-motile (B) and migratory (C) tumor cells. The rectangular box highlights migrating E-cad^{LO} cells. Scale bars, 50 μm.

(D) The percentage of protruding (left) and motile cells (right) plotted against E-cad status. Red lines indicate the median. The graph represents data from imaging fields with moving cells (11 out of 45 imaging fields from four mice, where symbols represent different mice).

Related to Figure S4 and Movies S1 and S2.

phenotype as indicated by E-cad expression (Figure S3B). This reversibility is not necessarily dependent on cell division, since sorted E-cad^{LO} cells plated into a 3D matrix and stained with a CellTracker dye to visualize cell division, reverted to an epithelial state both before (Figure S3C, upper) and after cell division (Figure S3C, lower). Combined, these results show that the mesenchymal state of E-cad^{LO} cells is plastic and can be gained and lost by tumor cells.

Similar to previously identified invasive signatures of tumor cells (Wang et al., 2004, 2007), many categories of E-cad^{LO} gene set were related to tissue development, morphogenesis, migration, and adhesion (Figures S3D–S3F). This result prompted us to visualize the behavior of these E-cad^{HI} and E-cad^{LO} tumor cells in vivo using multi-photon microscopy. To exclude YFP expression in non-epithelial lineages, tumors were imaged that developed upon transplantation of E-cad^{HI} tumor cells into the mammary glands of wild-type mice (Figure 4A). In addition to endogenous mCFP-labeled E-cad and YFP, we visualized type I collagen by imaging the second harmonic generation signal. As reported previously (Wyckoff et al., 2007), we found that the migratory behavior of tumor cells in these genetic PyMT tumors is very heterogeneous: while no migratory cells were found in the majority of imaging fields (Figure 4B; Movie S1), we found many migratory cells in some imaging fields (Figure 4C; Movie S2; in Figure S4A we demonstrate that cell motility is not due to Z-drift of the focal plane). The tumor cells migrated either individually or as streams in which single cells appeared to follow each other's migration path (Figure 4C), as has been demonstrated before in other tumor models (Patsialou et al., 2013; Roussos et al., 2011), but collective migration of cohesive epithelial clusters was not observed in this model. While on average E-cad^{HI}

Please cite this article in press as: Beerling et al., Plasticity between Epithelial and Mesenchymal States Unlinks EMT from Metastasis-Enhancing Stem Cell Capacity, Cell Reports (2016), http://dx.doi.org/10.1016/j.celrep.2016.02.034

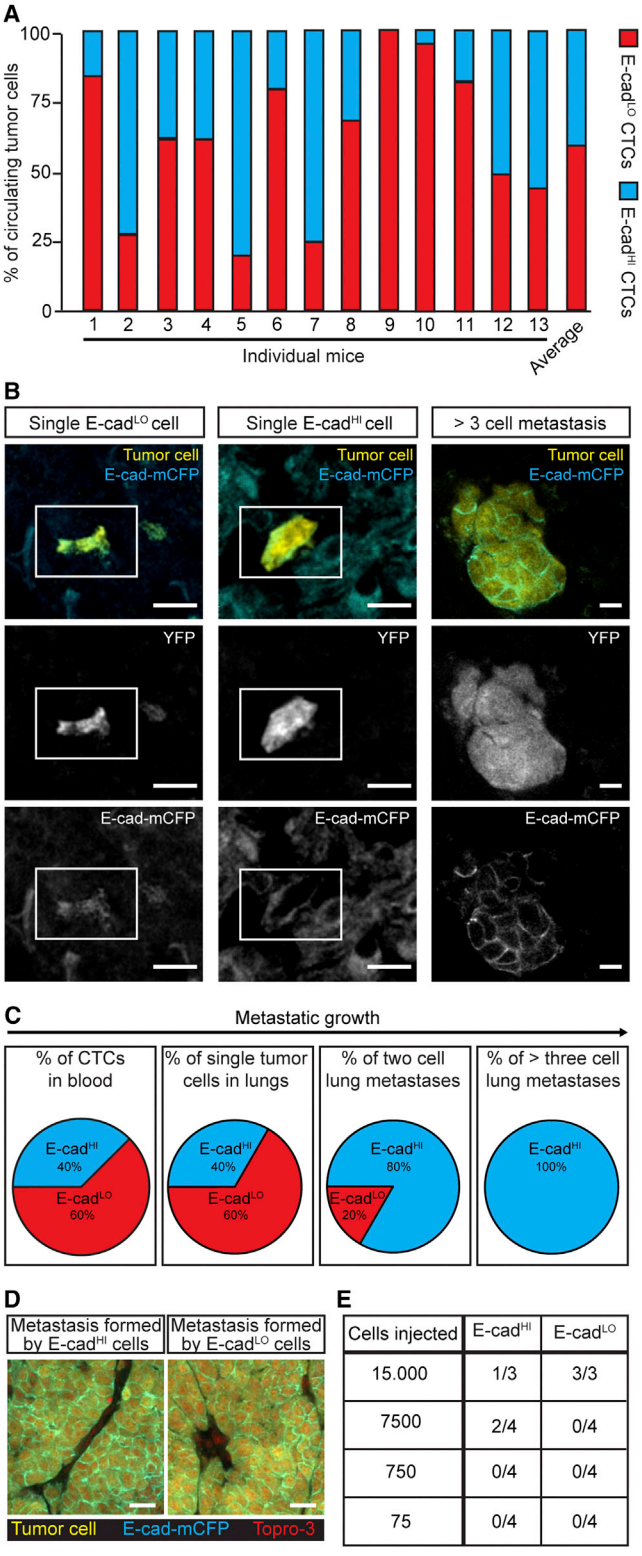

Cells injected	E-cad^{HI}	E-cad^{LO}
15.000	1/3	3/3
7500	2/4	0/4
750	0/4	0/4
75	0/4	0/4

Figure 5. Epithelial-Mesenchymal Plasticity Renders Potential Stem Cell Differences Irrelevant for Metastatic Outgrowth

(A) The percentage of E-cad^{LO}- and E-cad^{HI}-circulating tumor cells. n = 13 mice.

(B) Representative images of single E-cad^{LO} and E-cad^{HI} cells and a multicellular metastasis in the lung. White rectangle highlights single cells. Scale bars, 20 μm.

(C) Percentages of E-cad^{LO} and E-cad^{HI} tumor cells in blood and lungs. Blood: n = 13 mice; lungs: n = 143 metastases in 16 mice.

(D) Representative images of liver metastases grown from E-cad^{HI} cells (left) and E-cad^{LO} cells (right). Scale bars, 40 μm.

(E) Table indicating the metastatic outgrowth potential of E-cad^{LO} and E-cad^{HI} cells. Tumor-initiating cell frequency as tested by the Elda-limiting dilution test: E-cad^{HI} cells 1/21,228; E-cad^{LO} cells 1/17,545, p = 0.82.

Related to Figure S5.

cells were non-motile, the rare E-cad^{LO} cells were either protruding or displaying migratory behavior (Figure 4D). These migratory E-cad^{LO} cells do not relate to the CK14-positive cells (Figures S4B and S4C) that lead collective migration in organoids (Cheung et al., 2013). Collectively, our data show that E-cad^{LO} cells represent a rare population of motile cells that have undergone spontaneous EMT without experimental induction, within otherwise non-motile epithelial tumors.

Since we found that the small population of migratory cells in tumors has undergone EMT, we questioned whether these tumor cells enter the circulation in this mesenchymal state only or whether they can revert and/or enter in an epithelial state. Despite a large variation between mice regarding the total number of CTCs and the percentage of E-cad^{HI} and E-cad^{LO} CTCs, both types of CTCs were present in the blood of tumor-bearing MMTV-PyMT mice (Figure 5A). Next, we tested whether the E-cad^{LO}-circulating tumor cells show the same expression profile as the E-cad^{LO} tumor cells in the primary tumor. We performed single-cell sequencing and observed that the circulating E-cad^{LO} and E-cad^{HI} cells cluster into two populations and that the circulating E-cad^{LO} cells show the same expression profile as the primary E-cad^{LO} tumor cells (Figures S5A and S5B). Since in this mouse model tumor cells do not stay long enough in the circulation to switch to another state (99.99% of IV-injected tumor cells get cleared from circulation within 30 s [Figure S5C]), we can conclude from our data that disseminating tumor cells that enter the circulation are in a mesenchymal, but also an epithelial, state.

Next, we investigated the epithelial and mesenchymal state of endogenous spontaneous metastases to the lung. In line with the percentages of E-cad^{HI} and E-cad^{LO} cells in the blood, 40% of single metastasized tumor cells appeared to be E-cad^{HI} cells, and 60% were E-cad^{LO} cells (Figures 5B and 5C). In contrast to findings in prior studies in which EMT was induced (Stoletov et al., 2010), our data suggest that naturally occurring EMT does not influence the arrival and extravasation of the CTCs at the site of metastatic outgrowth. To investigate the cells that grow out to metastases, we examined endogenous metastases with a size of two and more than three cells. Although 20% of the two-cell micrometastases were E-cad negative, all metastases larger than three cells were E-cad positive (Figures 5C and 5D).

Since our histological analysis shows that all metastases larger than three cells contain E-cad^{HI} cells, we hypothesized that either only E-cad^{HI} cells are able to grow metastases or E-cad^{LO} cells convert to an epithelial state during the first cell divisions. Interestingly, E-cad^{HI} and E-cad^{LO} cells do not differ in their proliferative capacity (Figures S5D and S5E). To further

test the impact of each state, and especially epithelial-mesenchymal plasticity, on metastatic potential, we investigated the ability of E-cad^{HI} and E-cad^{LO} cells to initiate liver metastases. In contrast to previous reports with fixed states (Fantozzi et al., 2014; Ocaña et al., 2012; Shibue and Weinberg, 2009, 2011; Tsai et al., 2012), the potential to grow metastases from plastic E-cad^{HI} cells and E-cad^{LO} cells is approximately equal (Figure 5E). The outgrowth of epithelial metastases from the E-cad^{LO} cells strongly suggest that at least a significant fraction of the spontaneous metastases as found in Figure 5B are grown from mesenchymal E-cad^{LO} cells that have converted to an epithelial state during the first few cell divisions. Considering all these data together, we conclude that, although intrinsically epithelial and mesenchymal cells may differ in their stem cell potential, this difference does not provide a large metastatic outgrowth advantage as mesenchymal cells adapt an epithelial state after the first few cell divisions, thereby abolishing any potential initial differences in stem cell properties.

Collectively, our data provide evidence for the existence of EMT in vivo without experimentally altering EMT-inducers. Artificial interference of EMT regulators does not reflect the moderate fluctuations of expression levels that occurs under physiological conditions and therefore is likely to lead to more extreme phenotypes. Moreover, these manipulations artificially keep cells in fixed states, whereas we here show that cells adapt transient and reversible states. Our data support the notion that temporal acquisition of the mesenchymal state is important for migration, but not for entering the circulation. We observed that mesenchymal cells that arrive at the secondary site adapt an epithelial state after a few cell divisions. These cells therefore acquire the same stemness properties as their epithelial counterparts. Thus, due to epithelial-mesenchymal plasticity, any differences in stemness between epithelial and mesenchymal states will be lost and become irrelevant for metastatic outgrowth. In conclusion, we have demonstrated plasticity between epithelial and mesenchymal states, thereby ruling out a critical role for differential stemness capacities and ultimately the potential to grow metastases.

EXPERIMENTAL PROCEDURES

Mice

All experiments were carried out in accordance with the guidelines of the Animal Welfare Committee of the Royal Netherlands Academy of Arts and Sciences, the Netherlands. For more details, see the Supplemental Experimental Procedures.

Human Material

Human tissues were obtained in compliance with Dutch law that does not require informed consent when leftover materials are used anonymously.

Flow Cytometry on Mouse Material

After putting cells through a 70-μm strainer cap (BD Falcon), cells were sorted on a fluorescence-activated cell sorting AriaII special-ordered research product (BD Biosciences). The sort strategy is illustrated in Figure S1B. For more details, see the Supplemental Experimental Procedures.

Intravital Imaging

Imaging was performed on an inverted Leica TCS SP5 AOBS multi-photon microscope with a chameleon Ti:Sapphire pumped Optical Parametric Oscillator (Coherent). For more details, see the Supplemental Experimental Procedures.

ACCESSION NUMBERS

The accession number for the mRNA sequencing data reported in this paper has been uploaded to European Nucleotide Archive: PRJEB5939. The accession number for the single-cell mRNA sequencing data reported in this paper has been uploaded to GEO: GSE77107.

SUPPLEMENTAL INFORMATION

Supplemental Information includes Supplemental Experimental Procedures, five figures, one table, and two movies and can be found with this article online at http://dx.doi.org/10.1016/j.celrep.2016.02.034.

AUTHOR CONTRIBUTIONS

E.B., D.S., N.V., and J.v.R. designed the experiments. E.B., D.S., C.M., R.S., and P.v.D. performed the experiments. E.B., D.S., and N.V. analyzed the data. E.d.W. analyzed the mRNA deep-sequencing data. L.K. performed single-cell sequencing experiments. A.v.O. and L.K. analyzed the single-cell sequencing experiments. D.v.d.V., P.v.D., and E.V. helped to obtain patient material. E.B., D.S., E.d.W., N.V., and J.v.R. wrote the manuscript. J.v.R. conceived of the conceptual ideas and supervised the study.

ACKNOWLEDGMENTS

We would like to thank Anko de Graaff, Stefan van der Elst, Reinier van der Linden, and Rinske Drost for technical assistance, Hans Clevers and Hugo Snippert for mice, and the NKI/AVL Core Facility Molecular Pathology & Biobanking (CFMPB) of the NKI/AVL Biobank for material and lab support. This work was supported by NWO (91710330, 700.10.402, 175.010.2007.00, and 834.11.002), ERC (648804), and KWF (HUBR 2009-4621).

Received: September 16, 2015
Revised: December 16, 2015
Accepted: February 2, 2016
Published: March 3, 2016

REFERENCES

Beck, B., Lapouge, G., Rorive, S., Drogat, B., Desaedelaere, K., Delafaille, S., Dubois, C., Salmon, I., Willekens, K., Marine, J.C., and Blanpain, C. (2015). Different levels of Twist1 regulate skin tumor initiation, stemness, and progression. Cell Stem Cell *16*, 67–79.

Bill, R., and Christofori, G. (2015). The relevance of EMT in breast cancer metastasis: correlation or causality? FEBS Lett. *589*, 1577–1587.

Bukholm, I.K., Nesland, J.M., and Børresen-Dale, A.L. (2000). Re-expression of E-cadherin, alpha-catenin and beta-catenin, but not of gamma-catenin, in metastatic tissue from breast cancer patients [seecomments]. J. Pathol. *190*, 15–19.

Cheung, K.J., Gabrielson, E., Werb, Z., and Ewald, A.J. (2013). Collective invasion in breast cancer requires a conserved basal epithelial program. Cell *155*, 1639–1651.

Del Pozo Martin, Y., Park, D., Ramachandran, A., Ombrato, L., Calvo, F., Chakravarty, P., Spencer-Dene, B., Derzsi, S., Hill, C.S., Sahai, E., and Malanchi, I. (2015). Mesenchymal cancer cell-stroma crosstalk promotes niche activation, epithelial reversion, and metastatic colonization. Cell Rep. *13*, 2456–2469.

Fantozzi, A., Gruber, D.C., Pisarsky, L., Heck, C., Kunita, A., Yilmaz, M., Meyer-Schaller, N., Cornille, K., Hopfer, U., Bentires-Alj, M., and Christofori, G. (2014). VEGF-mediated angiogenesis links EMT-induced cancer stemness to tumor initiation. Cancer Res. *74*, 1566–1575.

Fischer, K.R., Durrans, A., Lee, S., Sheng, J., Li, F., Wong, S.T., Choi, H., El Rayes, T., Ryu, S., Troeger, J., et al. (2015). Epithelial-to-mesenchymal transition is not required for lung metastasis but contributes to chemoresistance. Nature *527*, 472–476.

Please cite this article in press as: Beerling et al., Plasticity between Epithelial and Mesenchymal States Unlinks EMT from Metastasis-Enhancing Stem Cell Capacity, Cell Reports (2016), http://dx.doi.org/10.1016/j.celrep.2016.02.034

Guy, C.T., Cardiff, R.D., and Muller, W.J. (1992). Induction of mammary tumors by expression of polyomavirus middle T oncogene: a transgenic mouse model for metastatic disease. Mol. Cell. Biol. *12*, 954–961.

Hanahan, D., and Weinberg, R.A. (2011). Hallmarks of cancer: the next generation. Cell *144*, 646–674.

Jeschke, U., Mylonas, I., Kuhn, C., Shabani, N., Kunert-Keil, C., Schindlbeck, C., Gerber, B., and Friese, K. (2007). Expression of E-cadherin in human ductal breast cancer carcinoma in situ, invasive carcinomas, their lymph node metastases, their distant metastases, carcinomas with recurrence and in recurrence. Anticancer Res. *27* (*4A*), 1969–1974.

Kalluri, R., and Weinberg, R.A. (2009). The basics of epithelial-mesenchymal transition. J. Clin. Invest. *119*, 1420–1428.

Kowalski, P.J., Rubin, M.A., and Kleer, C.G. (2003). E-cadherin expression in primary carcinomas of the breast and its distant metastases. Breast Cancer Res. *5*, R217–R222.

Lim, J., and Thiery, J.P. (2012). Epithelial-mesenchymal transitions: insights from development. Development *139*, 3471–3486.

Lin, E.Y., Jones, J.G., Li, P., Zhu, L., Whitney, K.D., Muller, W.J., and Pollard, J.W. (2003). Progression to malignancy in the polyoma middle T oncoprotein mouse breast cancer model provides a reliable model for human diseases. Am. J. Pathol. *163*, 2113–2126.

Mani, S.A., Guo, W., Liao, M.J., Eaton, E.N., Ayyanan, A., Zhou, A.Y., Brooks, M., Reinhard, F., Zhang, C.C., Shipitsin, M., et al. (2008). The epithelial-mesenchymal transition generates cells with properties of stem cells. Cell *133*, 704–715.

Morel, A.P., Lièvre, M., Thomas, C., Hinkal, G., Ansieau, S., and Puisieux, A. (2008). Generation of breast cancer stem cells through epithelial-mesenchymal transition. PLoS ONE *3*, e2888.

Ocaña, O.H., Córcoles, R., Fabra, A., Moreno-Bueno, G., Acloque, H., Vega, S., Barrallo-Gimeno, A., Cano, A., and Nieto, M.A. (2012). Metastatic colonization requires the repression of the epithelial-mesenchymal transition inducer Prrx1. Cancer Cell *22*, 709–724.

Onder, T.T., Gupta, P.B., Mani, S.A., Yang, J., Lander, E.S., and Weinberg, R.A. (2008). Loss of E-cadherin promotes metastasis via multiple downstream transcriptional pathways. Cancer Res. *68*, 3645–3654.

Patsialou, A., Bravo-Cordero, J.J., Wang, Y., Entenberg, D., Liu, H., Clarke, M., and Condeelis, J.S. (2013). Intravital multiphoton imaging reveals multicellular streaming as a crucial component of in vivo cell migration in human breast tumors. Intravital *2*, e25294.

Roussos, E.T., Balsamo, M., Alford, S.K., Wyckoff, J.B., Gligorijevic, B., Wang, Y., Pozzuto, M., Stobezki, R., Goswami, S., Segall, J.E., et al. (2011). Mena invasive (MenaINV) promotes multicellular streaming motility and transendothelial migration in a mouse model of breast cancer. J. Cell Sci. *124*, 2120–2131.

Shibue, T., and Weinberg, R.A. (2009). Integrin beta1-focal adhesion kinase signaling directs the proliferation of metastatic cancer cells disseminated in the lungs. Proc. Natl. Acad. Sci. USA *106*, 10290–10295.

Shibue, T., and Weinberg, R.A. (2011). Metastatic colonization: settlement, adaptation and propagation of tumor cells in a foreign tissue environment. Semin. Cancer Biol. *21*, 99–106.

Snippert, H.J., van der Flier, L.G., Sato, T., van Es, J.H., van den Born, M., Kroon-Veenboer, C., Barker, N., Klein, A.M., van Rheenen, J., Simons, B.D., and Clevers, H. (2010). Intestinal crypt homeostasis results from neutral competition between symmetrically dividing Lgr5 stem cells. Cell *143*, 134–144.

Srinivas, S., Watanabe, T., Lin, C.S., William, C.M., Tanabe, Y., Jessell, T.M., and Costantini, F. (2001). Cre reporter strains produced by targeted insertion of EYFP and ECFP into the ROSA26 locus. BMC Dev. Biol. *1*, 4.

Stoletov, K., Kato, H., Zardouzian, E., Kelber, J., Yang, J., Shattil, S., and Klemke, R. (2010). Visualizing extravasation dynamics of metastatic tumor cells. J. Cell Sci. *1*, 2332–2341.

Thiery, J.P., and Sleeman, J.P. (2006). Complex networks orchestrate epithelial-mesenchymal transitions. Nat. Rev. Mol. Cell Biol. *7*, 131–142.

Tsai, J.H., Donaher, J.L., Murphy, D.A., Chau, S., and Yang, J. (2012). Spatiotemporal regulation of epithelial-mesenchymal transition is essential for squamous cell carcinoma metastasis. Cancer Cell *22*, 725–736.

Wang, W., Goswami, S., Lapidus, K., Wells, A.L., Wyckoff, J.B., Sahai, E., Singer, R.H., Segall, J.E., and Condeelis, J.S. (2004). Identification and testing of a gene expression signature of invasive carcinoma cells within primary mammary tumors. Cancer Res. *64*, 8585–8594.

Wang, W., Wyckoff, J.B., Goswami, S., Wang, Y., Sidani, M., Segall, J.E., and Condeelis, J.S. (2007). Coordinated regulation of pathways for enhanced cell motility and chemotaxis is conserved in rat and mouse mammary tumors. Cancer Res. *67*, 3505–3511.

Wellner, U., Schubert, J., Burk, U.C., Schmalhofer, O., Zhu, F., Sonntag, A., Waldvogel, B., Vannier, C., Darling, D., zur Hausen, A., et al. (2009). The EMT-activator ZEB1 promotes tumorigenicity by repressing stemness-inhibiting microRNAs. Nat. Cell Biol. *11*, 1487–1495.

Welm, A.L., Sneddon, J.B., Taylor, C., Nuyten, D.S., van de Vijver, M.J., Hasegawa, B.H., and Bishop, J.M. (2007). The macrophage-stimulating protein pathway promotes metastasis in a mouse model for breast cancer and predicts poor prognosis in humans. Proc. Natl. Acad. Sci. USA *104*, 7570–7575.

Wyckoff, J.B., Wang, Y., Lin, E.Y., Li, J.F., Goswami, S., Stanley, E.R., Segall, J.E., Pollard, J.W., and Condeelis, J. (2007). Direct visualization of macrophage-assisted tumor cell intravasation in mammary tumors. Cancer Res. *67*, 2649–2656.

Yang, J., Mani, S.A., Donaher, J.L., Ramaswamy, S., Itzykson, R.A., Come, C., Savagner, P., Gitelman, I., Richardson, A., and Weinberg, R.A. (2004). Twist, a master regulator of morphogenesis, plays an essential role in tumor metastasis. Cell *117*, 927–939.

Yu, M., Bardia, A., Wittner, B.S., Stott, S.L., Smas, M.E., Ting, D.T., Isakoff, S.J., Ciciliano, J.C., Wells, M.N., Shah, A.M., et al. (2013). Circulating breast tumor cells exhibit dynamic changes in epithelial and mesenchymal composition. Science *339*, 580–584.

Zheng, X., Carstens, J.L., Kim, J., Scheible, M., Kaye, J., Sugimoto, H., Wu, C.C., LeBleu, V.S., and Kalluri, R. (2015). Epithelial-to-mesenchymal transition is dispensable for metastasis but induces chemoresistance in pancreatic cancer. Nature *527*, 525–530.